View Article Online
View Journal

Green Chemistry

Cutting-edge research for a greener sustainable future

Accepted Manuscript

This article can be cited before page numbers have been issued, to do this please use: D. K. Nguyen, T. Goculdas, M. A. Al Ismail, C. Kulp, S. Sadula and D. G. Vlachos, *Green Chem.*, 2026, DOI: 10.1039/D6GC03112A.

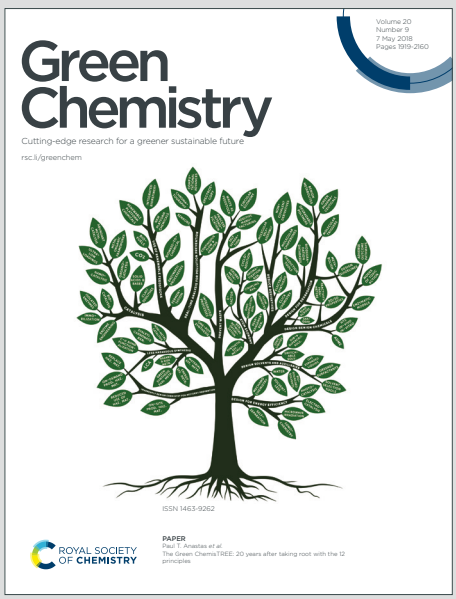

View Article Online
DOI: 10.1039/D6GC03112A

Green Foundation Box

1. This work presents a novel synthetic blueprint for producing high-performance anionic surfactants from a hybrid of post-consumer polyolefin plastics waste and lignocellulosic biomass, entirely avoiding fossil-derived feedstocks. By coupling electrified non-thermal plasma oxidation with mild organic transformations, the route replaces hazardous transition metal catalysts, strong oxidants, and energy-intensive processes typically required for surfactant synthesis.
2. The resulting plastics-derived oleo-furan and branched sulfonate surfactants achieved a critical micelle concentration of 591 ppm and a Krafft temperature below 0 °C, outperforming commercial linear alkylbenzene sulfonates and sodium lauryl sulfate. The overall process converts 1 mol of LDPE plastic waste into 0.31 mol of surfactant (31% molar efficiency) using electrical energy and oxygen.
3. Future improvements include optimizing the plasma reactor geometry and scale-up strategy to increase energy efficiency beyond the current 52%, extending the process to mixed plastic waste streams, improving furoate yields during esterification, and performing full life-cycle and techno-economic analyses to establish a pathway to cost-competitive, large-scale sustainable surfactant production.

View Article Online
DOI: 10.1039/D6GC03112A

Oleo-Furan and Branched Surfactants Made from Recycled and Renewable Feedstocks

*Darien K. Nguyen[†1,2], Tejas Goculdas[†1], Mahdi A. Al Ismail[1], Caroline Kulp[1], Sunitha Sadula[3], Dionisios G. Vlachos [*1,2,3]*

1 – Department of Chemical and Biomolecular Engineering, University of Delaware, Newark, Delaware 19716, United States

2 – Center for Plastics Innovation, University of Delaware, Newark, Delaware 19716, United States

3 – Delaware Energy Institute, University of Delaware, Newark, Delaware 19716, United States

† Contributed equally.

* Corresponding author: vlachos@udel.edu

KEYWORDS: Hybrid materials, plastics waste, biomass, upcycling, detergents

ABSTRACT

The widespread reliance on fossil-derived linear alkylbenzene sulfonates (LAS) in surfactant formulations presents significant sustainability and biodegradability challenges. We report a synthetic route to oleo-furan sulfonate (OFS) and branched sulfonate surfactants derived from a hybrid of renewable biomass and polyolefin plastics waste carbon. Plastics-derived paraffins were obtained via catalytic hydrogenolysis and subsequently oxidized using non-thermal atmospheric plasma. The resulting oxygenated paraffins, rich in mid-chain ketones and alcohols, were selectively reduced to mono-alcohols using sodium borohydride. These plastics-derived hydroxy paraffins were then coupled with biomass-derived 2-furoic acid to produce furoates and olefins, which were sulfonated to yield unique oleo-furan and branched sulfonate surfactants. The resulting surfactants exhibited superior performance, including a low critical micelle concentration (CMC) of 591 ppm and a Krafft temperature below 0 °C, surpassing not only previously synthesized OFS but also commercial LAS and sodium lauryl sulfates (SLS). This work offers a blueprint for producing high-value specialty surfactants from hybrid waste feedstocks and contributes to the advancement of circular, high-performance surfactant technologies.

View Article Online
DOI: 10.1039/D6GC03112A

INTRODUCTION

The specialty chemicals sector, currently valued at over $600 billion, and sourced primarily from fossil fuel feedstocks[1, 2], is expected to continue growing. As the industry grows, so does the need to make products from renewable carbon sources, especially in large volume sectors like surfactants[3]. Surfactants are ubiquitous ingredients in cleaning, personal care, and industrial formulations[4]. Among them, linear alkylbenzene sulfonates (LAS) dominate due to their strong detergency[5]. Fossil-based LAS derived from benzenes and long-chain alkanes[6] suffer from poor anaerobic biodegradability, high Kraft temperatures, and low calcium tolerance, which often necessitate formulation additives like ethylenediaminetetraacetic acid (EDTA)[7, 8] that increase the cost. Replacing them with high-performance alternatives is a critical priority.

Oleo-furan sulfonates (OFS) can be such a replacement[8, 9]. They feature a biobased furan ring as the polar headgroup and a long-chain alkyl tail, often derived from fatty acids. This amphiphilic structure mimics LAS, offering strong calcium tolerance, low Kraft temperatures, and favorable biodegradability, due to the polar furan ring providing superior water solubility[10, 11]. However, fatty acids are produced in small quantities from edible oils, which are heavily used in the food and cosmetic industry. Their recycled products are used for biodiesel and jet fuels[11, 12]. Technologically, C–C coupling between furans and fatty acids is challenging, requiring either high temperature ketonization[13, 14] or stoichiometric amounts of corrosive trifluoroacetic acid under milder acylation conditions[8]. These challenges in the process and raw materials highlight a need for new synthetic strategies and carbon sources.

Post-consumer plastics waste presents a compelling feedstock due to its massive scale and under-recycling[15, 16]. The joint valorization of biomass and plastics waste feedstocks could contribute to long-term sustainability[17, 18]. However, polyolefins, the most abundant plastics, are chemically inert[19]. Upcycling plastics has predominantly focused on catalytic thermal decomposition to liquid fuels and waxy hydrocarbons[20-23]. These feedstocks and products lack functional groups for further co-processing. Current strategies for activating these feedstocks, such as traditional catalytic oxidation reactions, require high loadings of expensive transition metal catalysts, elevated temperatures, hazardous solvents, and strong oxidants (e.g., hydrogen peroxide and other acids), making them typically unsustainable[24]. In contrast, non-thermal plasma can drive the oxidation reaction solely using electrical energy, without the need for toxic gases, solvents, or catalysts.

This study presents a novel process for synthesizing oleo-furan and branched sulfonate surfactants using biomass-derived 2-furoic acid and plastics-derived paraffins (**Scheme 1)**. The paraffins were obtained via catalytic hydrogenolysis of polyethylene and subsequently functionalized into oxygenates, primarily mono-ketones and alcohols, using non-thermal, atmospheric plasma. These oxygenated paraffins were then reduced with sodium borohydride to form alcohols, which were co-processed with 2-furoic acid, a biomass derivative, to generate furoates and olefins. The resulting furoates and olefins were sulfonated to produce unique oleo-furan and branched sulfonate surfactants. These surfactants exhibit superior performance characteristics, including low critical micelle concentrations (CMC) and low Krafft temperatures, compared to previously synthesized OFS and commercial surfactants. Overall, this work offers a promising blueprint for producing high-performance surfactants from hybrid biomass and plastics waste feedstocks.

View Article Online
DOI: 10.1039/D6GC03112A

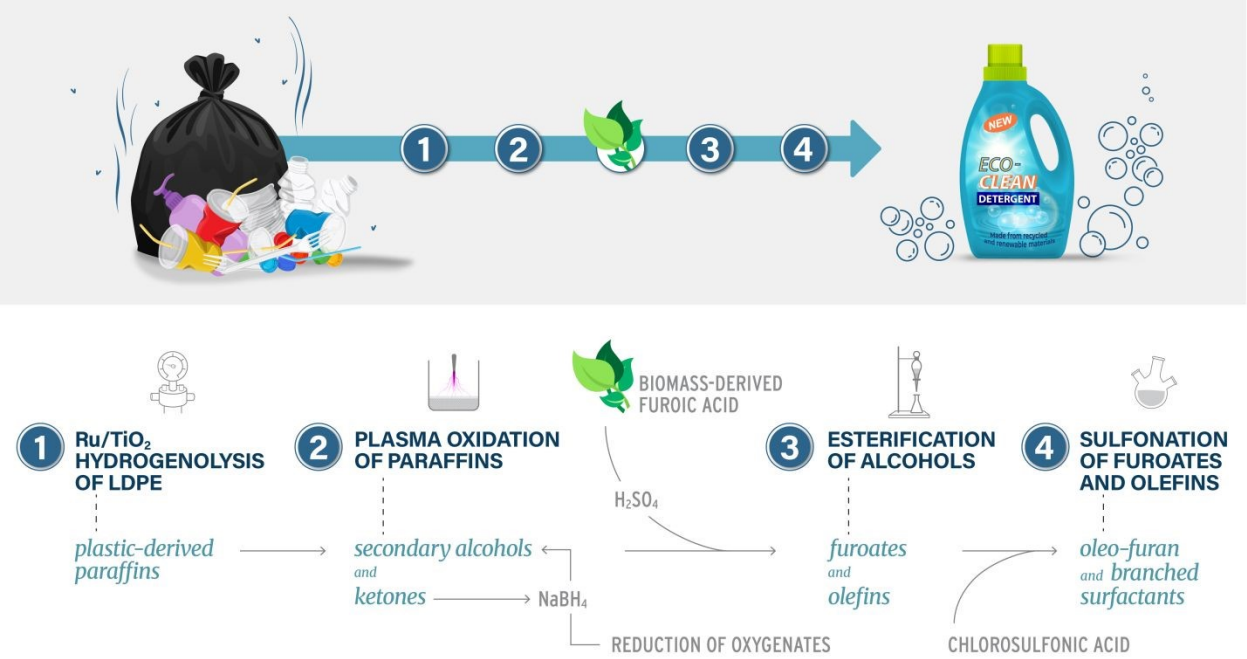

Scheme 1. *Illustration of the pathway to surfactants from hybrid feedstock.*

MATERIALS AND METHODS

Chemicals

Oxygen (99.997%) and helium (99.999%) gases were purchased from KeenGas. Hexanes, *n*-dodecane (99%), *n*-decane (99%), *n*-tetradecane (99%), *n*-hexadecane (99%), 2-dodecanol (99%), 2-dodecanone (98%), 1-hexandecanol (99%), 3-hexadecanone (98%), low-density polyethylene (LDPE, weight-average molecular weight {M_w} ~4 kg/mol), methylene chloride (> 99.8%), acetonitrile (> 99.9%), methanol (> 99.9%), 2-octanol (> 97%), 2-nonanol(> 98%), 5-nonanol (> 98%), sodium borohydride acetonitrile (> 99.9%), tetrahydrofuran (> 99.9%), ruthenium nitrosyl nitrate $Ru(NO)(NO_3)_3$ solution in diluted HNO_3 (Sigma-Aldrich no. 373567), 2-furoic acid (98%), octyl-2-furoate, chlorosulfonic acid (98%), and anhydrous chloroform were purchased from Sigma-Aldrich. Sulfuric acid (98%), ethyl acetate, diethyl ether, sodium bicarbonate were obtained from Fisher Scientific. TiO_2 nanopowder (99.5%, 5 nm, anatase) was obtained from US Research Nanomaterials.

Hydrogenolysis of LDPE over Ru/TiO_2 Catalyst

The Ru/TiO_2 catalyst was prepared using the wetness impregnation method[25]. TiO_2 nanopowder (99.5%, US Research Nanomaterials, 5 nm, anatase) was first calcined at 450 °C for 4 h in air. The support was placed in a 50 ml beak and heated to 70 °C with the subsequent addition of ruthenium nitrosyl nitrate $Ru(NO)(NO_3)_3$ solution in diluted HNO_3 (Sigma-Aldrich no. 373567). The suspension was vigorously stirred with a glass rod for 1.5 h until complete dryness; then, it was stored in an oven at 100 °C for 12 h. Before the reaction, the catalyst was reduced in the flow of 50% H_2/He at 300 °C for 2 h (ramping rate 10 °C/min).

Hydrogenolysis of LDPE (4 kg/mol) was conducted to yield plastics-derived paraffins (PDP). 3.4 g of LDPE, 0.1 g of Ru/TiO_2 catalyst, and a stir bar was added into a 50 mL Parr reactor. The Parr reactor was pressurized with 30 bar of H_2. The reaction was conducted at 250 °C for approximately 4 h. The resulting products were filtered and collected in dichloromethane. The

View Article Online
DOI: 10.1039/D6GC03112A

solution was rotovapped at 125 mbar for 30 min at 40 °C to remove dichloromethane and volatile alkanes ($<C_8$).

Plasma Reactor and Diagnostics

Plasma oxidation of the PDP was carried out in a pin-to-plate reactor configuration[26] of an enlarged glass diameter to increase the production rate. Approximately 600 mg of hydrogenolysis wax was placed at the bottom of a glass reactor (27 mm diameter), which was slightly heated (35 ºC) using an external hotplate to create a melt. To maintain a controlled gas atmosphere, a helium (490 sccm) and oxygen (10 sccm) gas mixture was introduced via mass flow controllers (Brooks GF 40 series). A high-voltage stainless-steel pin was suspended above the melted wax surface, while a grounded stainless-steel plate was positioned at the exterior bottom of the glass vessel. The gap between the pin and the plate was 7 mm, with the hydrogenolysis wax and glass vessel serving as dielectrics. Non-thermal, atmospheric-pressure plasma was generated using a direct current (DC) micro-pulsed high-voltage power supply (HVPPS1160). The peak-to-peak voltage, frequency, and duty cycle were maintained at 9 kV, 5 kHz, and 1%, respectively, resulting in a calculated dissipated power of approximately 2.2 W.

Voltage and current signals were recorded using a high-voltage probe (Tektronix P6015) and a current monitor (Pearson 6585), respectively. Both signals were acquired in real time using a Tektronix MDO32 wideband oscilloscope. A representative oscillogram is shown in **Figure S1**. The average dissipated power (i.e., the power consumed by the plasma discharge) was calculated using the following equation:

$$P = \frac{1}{T_p}\int_0^{T_p} \mathrm{v}(t)i(t)dt \qquad (1)$$

where T_p is the period of each wave, and *v(t)* and *i(t)* are the time-dependent voltage and current, respectively.

Optical emission spectroscopy (OES) measurements were performed using an AvaSpec-ULS4096CL-EVO spectrometer (Avantes). Light emission from the plasma was collected using a 400 μm optical fiber, and the wideband emission spectrum in the 300–900 nm range was recorded and analyzed using Avasoft software. A representative emission spectrum of the He/O_2 discharge is shown in **Figure S2**.

Separation and Extraction of Plastics-Derived Oxygenated Paraffins (PDOP)

PDOP were extracted from the unreacted *n*-alkanes using a method similar to that described previously[27]. A mixture of acetonitrile and methanol (4:1 v/v) was added to the plasma-treated PDP, achieving a solvent-to-solute ratio of 4:1 v/v. This solution was sonicated (Branson 1800) for 15 min to facilitate the extraction of oxygenates from the wax phase into the polar solvent phase. Following sonication, the resulting cloudy solution typically phase-separated in a separatory funnel after ~4–6 h. To accelerate the liquid–liquid extraction and enhance the purification of oxygenates, the cloudy solution was centrifuged (Eppendorf Centrifuge 5425) in 2 mL centrifuge tubes for 10 min at 10,000 rpm. The polar phase was then easily separated from the non-polar wax phase. Both phases were subsequently rotovapped at 175 mbar for 30 min at 40 °C to remove residual acetonitrile and methanol. The non-polar phase, containing unreacted waxes, could be recycled back into the plasma reactor for further oxidation.

Sodium Borohydride Reduction

In a typical procedure[28], 2 equivalents of $NaBH_4$ (250 mg, 6.7 mmol), dissolved in 10 ml of $MeOH/H_2O$ (50/50) mixture, were added in portions to a suspension of the PDOP (1 g, ~3.3 mmol oxygenates) in methanol (20 ml) at 0 °C. The mixture was brought to room temperature after the initial effervescence and stirred for 2 h. The reaction was quenched with a solution of ammonium chloride (15 ml) at 0 °C and concentrated in a vacuum. The residue was diluted with ethyl acetate

View Article Online
DOI: 10.1039/D6GC03112A

(80 ml), washed with 2 aliquots of saturated aqueous $NaHCO_3$ (2 x 20 ml) and brine, dried over Na_2SO_4, filtered, and concentrated in a vacuum.

Esterification

The esterification reaction[9] was conducted by first preheating a hot plate to 150 °C. A small stir bar was placed in each 10 ml crimp-neck glass vial, followed by the addition of 0.01388 moles of alcohol (typically 5-nonanol) and 0.01388 moles of 2-furoic acid. After all reactants were introduced, one mole percent of the catalyst (typically sulfuric acid) was added to each vial, which was then sealed with a crimp vial cap. The sealed vials were placed in a 150 °C mineral oil bath and heated for 1–3 h. To facilitate water removal, a syringe was used to pierce the vial caps and extract any water formed during the reaction at 15-min intervals. Once the reaction was complete, the vials were transferred to an ice bath to quench the reaction. The reaction mixture was then rinsed and transferred into a clean 20 mL vial using a 50:50 mixture of ethyl acetate and cyclohexane as the solvent. The total volume of the solvent and reaction product was recorded. To prepare samples for gas chromatography (GC) analysis, the rinsed reaction solution was combined with an additional 50:50 cyclohexane and ethyl acetate mixture, along with eicosane as an internal standard.

Sulfonation

The plastics-derived furoates and olefins (PDFO), including the reference (octyl-2-furoate), was sulfonated and neutralized to make a mixture of plastics-derived oleo-furan and branched sulfonate (PDOFBS) surfactants[9]. The crude mixture (0.5 g, ~1.6 mmol assuming tetradecyl-2-furoate) was added to anhydrous chloroform (5 mL) and mixed until homogeneous. 1 equiv. of chlorosulfonic acid was added and the produced HCl was bubbled into a water trap, confirming reaction progression. The reaction was complete after bubbling stopped. The resulting mixture was rotary evaporated to remove chloroform, leading to a dark green/purple liquid. The resulting liquid was diluted in water and neutralized with saturated aqueous $NaHCO_3$ to attain a neutral pH (7). Cold acetone was added into the solution to precipitate out $NaHCO_3$ and was separated out via filtration. Acetone was removed via rotary evaporation, leaving the resulting water solution with sulfonated products. To remove any unreacted alkanes, esters, or olefins, cyclohexane was added for liquid-liquid extraction. The aqueous layer was evaporated leaving the resulting purified sulfonate surfactants.

Characterization of Surfactants

Sulfonated surfactants, sulfonated octyl-2-furoate standard and PDOFBS, were characterized for Krafft temperature and critical micelle concentration (CMC). CMC was identified using a Sigma 700 Surface Tension attached with a Du Nouy Ring. The average and standard deviation surface tension of 10 measurements at varying concentrations of the surfactant (0.3 – 15000 ppm) in 18.2 Mohm DI water were collected at room temperature. The CMC is calculated as the point of intersection between the initial decreasing slope and the plateau of the surface tension vs. ln(C) plot.

The Krafft temperature was determined by analyzing the conductivity of the surfactants (slightly above CMC) over various temperatures (1 – 20 °C). The Krafft point is denoted as a temperature accompanied by a sharp increase/decrease in conductivity due to the dissolution or precipitation of the anionic surfactant in DI water. Cooling of the solution was conducted using a Stir-Kool (SK-24D-AW) cooling plate and the conductivity was measured using a conductivity meter (Oaklon, CON 110 Series). The average and standard deviation of triplicate conductivity values at each temperature were reported.

View Article Online
DOI: 10.1039/D6GC03112A

The Toxicity Estimation Software Tool (TEST), developed by EPA, was used to estimate the lethal concentration (LC_{50}) for the fathead minnow as well as the Log (K_{ow}) and bioconcentration factor for the surfactants. TEST is a peer-reviewed tool using QSAR (Quantitative Structure-Activity Relationship) to estimate chemical toxicity based on molecular descriptors, like molecular weight and hydrophilicity. TEST has been trained on datasets from ECOTOX, which contain various aliphatic and aromatic carbamates, esters, and sulfides structurally similar to the molecules analyzed. These calculations were supplemented with linear and non-linear BIOWIN biodegradability predictions from the Estimation Programs Interface (EPI) Suite. The EPI Suite software was developed by the US Environmental Protection Agency's Office of Pollution Prevention and Toxics and SRC, Inc. It is a screening-level tool, intended for use in applications such as rapid evaluation of chemicals for release potential and classifying chemicals for future investigation.

Product Analysis

Reaction products were analyzed using gas chromatography (GC), nuclear magnetic resonance (NMR) spectroscopy, and Fourier-transform infrared (FTIR) spectroscopy. For GC analysis, products were diluted in dichloromethane and analyzed using a flame ionization detector (GC-FID, Agilent 7890B) equipped with an Agilent J&W HP-INNOWax column (30 m, 0.25 mm, 0.25 μm). For ^{1}H-NMR spectroscopy, products were diluted in deuterated chloroform or deuterated water and analyzed on a NEO 400 MHz spectrometer equipped with a 5-mm BBFO probe. FTIR spectroscopy was performed directly on the products using a Nicolet iS50 spectrometer, coupled with a golden gate diamond attenuated total reflectance (ATR) module and an MCTB detector, at a resolution of 4.0 cm^{-1} with an average of 32 scans. Quantification of the products (n-alkanes and corresponding oxygenates) was performed using GC-FID with external standard calibrations based on known reference compounds, and response factors were extrapolated for compounds without available standards. Both the weight percent distribution of the mixtures and the yields were calculated. It should be noted that the yields of all quantified products from hydrogenolysis and plasma treatment do not sum to 100%, as volatile compounds ($<C_8$) were lost during the rotary evaporation step. The esterification products were quantified with a GC-FID equipped with an HP-1 column (Agilent). To assess the possible formation of lighter gaseous species and evaporative losses during plasma treatment, the outlet gas was bubbled through an acetone solvent trap in an ice bath and subsequently analyzed by GC.

RESULTS AND DISCUSSION

Hydrogenolysis of Plastics Waste to Plastics-Derived Paraffins (PDP)

To obtain PDP, hydrogenolysis of LDPE was carried out over Ru/TiO_2 (**Figure 1a**). This catalyst has demonstrated effectiveness in plastics conversion into liquid n-alkanes, with relatively short reaction times, and is easy to make[25, 29]. The hydrogenolysis products from multiple reaction batches were combined to ensure homogeneity and were analyzed using GC (**Figure 1b**). As expected, the majority of the PDP consisted of *n*-alkanes ranging from C_9 to C_{32}, along with a smaller yield of branched isomers, consistent with previous studies[32]. Lighter n-alkanes ($< C_9$) and the dichloromethane solvent were removed via rotary evaporation for easier subsequent processing (i.e., plasma oxidation). Product yields of desired hydrocarbons were calculated to be 73%, with the remaining 27% being lighter alkanes ($< C_9$) and methane (**Figure S3**). The final mixture contained approximately 75% *n*-alkanes and 25% isomers (**Figure 1c)**, with the distribution centered around C_{12}-C_{13}. This chain-length range is favorable for surfactant production.

View Article Online
DOI: 10.1039/D6GC03112A

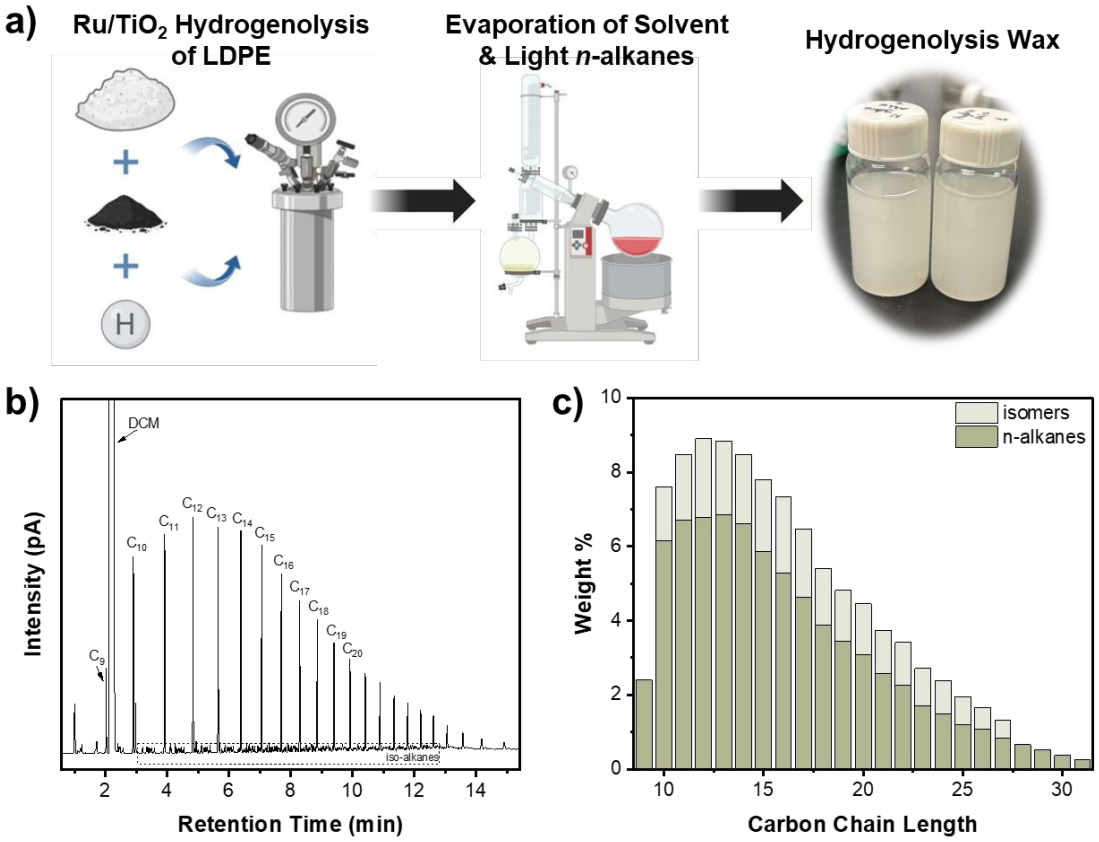

Figure 1. *(a) Process flow schematic of the hydrogenolysis of LDPE over Ru/TiO_2. (b) GC spectra of hydrogenolysis wax. (c) Weight percent distribution of n-alkanes and isomers of hydrogenolysis wax. Reaction conditions: catalyst-to-polymer ratio: 0.03, catalyst mass: 0.1 g, treatment time: 4 h, H_2 pressure: 30 bar, stir rate: 400 rpm, and temperature: 250 ºC. GC conditions: HP-Innowax column from 30 – 250 ºC in dichloromethane.*

Non-Thermal Plasma Oxidation of PDP to Plastics-Derived Oxygenated Paraffins (PDOP)

The PDP was plasma-treated in a pin-to-plate reactor to achieve plastic-derived oxygenated paraffins (PDOP) (**Figure 2a**). Mechanistically, oxygen plasma oxidizes aliphatic alkanes through hydrogen abstraction and subsequent radical recombination with reactive oxygen species[26, 30, 31], forming oxygenated hydrocarbons (**Figure 2b**). To establish proof of concept and ensure stability of the extracted oxygenates, the plasma treatment and oxygenate extraction were first performed on a model compound, hexadecane (*n*-C_{16}) (**Figure S4**). To maximize the yield of mono-oxygenates (e.g., mono-alcohols and mono-ketones) over secondary products (e.g., di-oxygenated or oligomerized species), the conversion was kept relatively low (~25%), yielding 18% of the desired oxygenates (72% selectivity). Notably, branched isomers are also susceptible to plasma oxidation and may be more reactive than linear alkanes due to the increased stability of tertiary vs. secondary radicals formed during hydrogen abstraction[32-35]; however, they are difficult to discern from oxygenated n-alkanes due to coelution.

Processing and quantifying the PDOP was challenging due to the large fraction of unreacted paraffins (~75%) and co-elution of oxygenated species with branched isomers (**Figure S5a**). Therefore, separation and extraction were implemented (Materials and Methods). In short, a mixture of acetonitrile and methanol was added to the PDOP for a one-stage liquid-extraction process, followed by evaporation of the polar solvent. The resulting PDOP (**Figure 2c**) comprised approximately 75% of oxygenates and 25% of *n*-alkanes, achieving an overall yield efficiency of

View Article Online
DOI: 10.1039/D6GC03112A

52%. Due to the co-elution of isomeric oxygenates derived from different alkane chain lengths (e.g., C_{12} alcohols eluting similarly to C_{13} ketones), precise quantification was difficult. Retention times were grouped based on standards, and all peak areas within each bin were attributed to a specific chain length (**Figure 2d**). The oxygenates ranged from C_8 to C_{23}, with the highest yields centered between C_{12} and C_{17}. Minimal conversion of longer-chain alkanes (above C_{23}) was observed, likely due to the higher reactivity and volatility of shorter-chain compounds within the plasma reactor[31]. Volatile C_9–C_{11} alkanes evaporated, as evidenced by their high concentration in the gas trap (**Figure S5b**) and their absence in the product mixture post-reaction. Overall yields of oxygenates from each reaction are shown in **Figure S6**. The non-polar phase, containing unreacted hydrocarbons recovered from extraction, was recycled back into the plasma reactor.

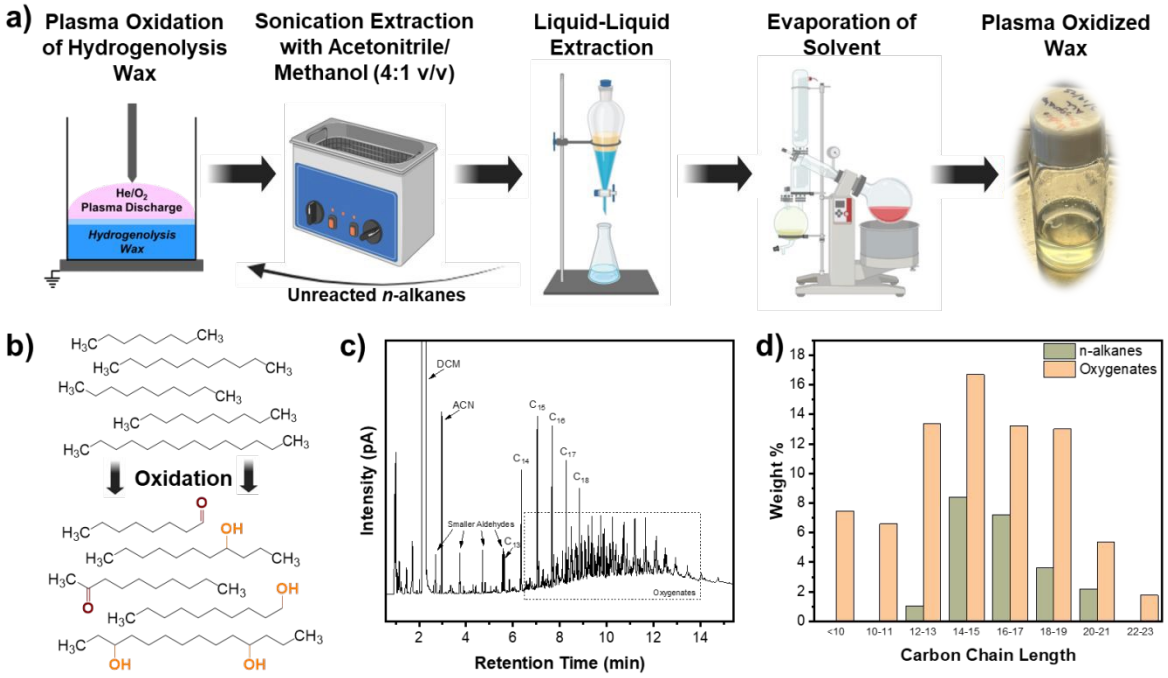

Figure 2. *(a) Process flow schematic of the plasma oxidation of hydrogenolysis wax and separation and extraction steps to obtain plasma-oxidized wax. (b) Schematic of plasma oxidation of hydrogenolysis wax (n-alkanes) to corresponding oxygenates. (c) GC spectra of plasma-oxidized wax. (c) Weight percent distribution of n-alkanes and oxygenates in plasma-oxidized wax. Plasma operating conditions: voltage: 9 kV, frequency: 5 kHz, O_2 feed molar percent: 2%, and temperature: 30 ºC. GC conditions: HP-Innowax column from 30 – 250 ºC in dichloromethane.*

Organic Transformations to Plastic-Derived Oleo-furan and Branched Sulfonates (PDOFBS)

In order to transform the PDOP into plastics-derived oleo-furan and branched sulfonates (PDOFBS), the process requires three organic transformations: reduction, esterification, and sulfonation. The optimization of these reactions and application to oxygenated plastics waste derivatives is described.

Sodium Borohydride Reduction: PDOP to Plastics-Derived Hydroxy Paraffins (PDHP)

As previously stated, the PDOP comprised a mixture of C_8-C_{22} oxygenates, evenly split between alcohols and carbonyls, mainly in the C_{12}-C_{17} range (**Figure 2d**). Carbonyls can undergo self-condensation reactions[36] and acetal formation[37] under acidic conditions during esterification and sulfonation. Therefore, to enrich mono-alcohols for surfactant synthesis and eliminate

View Article Online
DOI: 10.1039/D6GC03112A

condensation reactions, the PDOP required reduction to plastic-derived hydroxy paraffins (PDHP) (**Figure 3a**). However, due to the non-selective nature of plasma oxidation, the carbonyl group is positioned anywhere on the alkyl chains, with mostly secondary ketones. Pd/C, screened for hydrogenation, resulted in low conversion of the middle-chain model ketones (6-undecanone and 12-tricosanone, **Table S1**). Therefore, a sodium borohydride reduction method was utilized to reduce secondary ketones to alcohols, first testing its efficiency with 2-dodecanone and 6-undecanone models. As shown in **Table S2,** both ketones were completely converted to their corresponding alcohols. The reaction was also performed on an equimolar mixture of 2-dodecanone and 2-dodecanol to assess further how plastics-derived oxygenate streams may behave. The ketone was again fully reduced, and the initial alcohol remained intact. These results confirm the selective reduction of ketones in the presence of alcohols via sodium borohydride.

Using the same reaction conditions as the model compounds, around ~95% conversion of PDOP to PDHP was confirmed by GC and FTIR (**Figure 3**). GC spectra showed a clear consolidation of peaks corresponding to alcohols across various alkane chain lengths (**Figure S7a**), with a distribution centered around C_{12}–C_{17} (**Figure 3b**), consistent with the pre-reduction oxygenate profile. ATR-FTIR (**Figure 3c)** analysis revealed a clear reduction in the sharp absorption band at 1720 cm^{-1}, associated with C=O stretching vibrations, and an increase in the broad band at 3400 cm^{-1}, corresponding to O–H stretching. Additionally, ^{1}H-NMR analysis (**Figure S7b**) further indicated that oxygen-containing aldehyde (~9.5 ppm) and ketone (~2.3 ppm) signals decreased significantly, while the alcohol peak (~3.8-4 ppm) increased. These results successfully demonstrate the selective reduction of ketones and aldehydes to alcohols in the mixed PDOP.

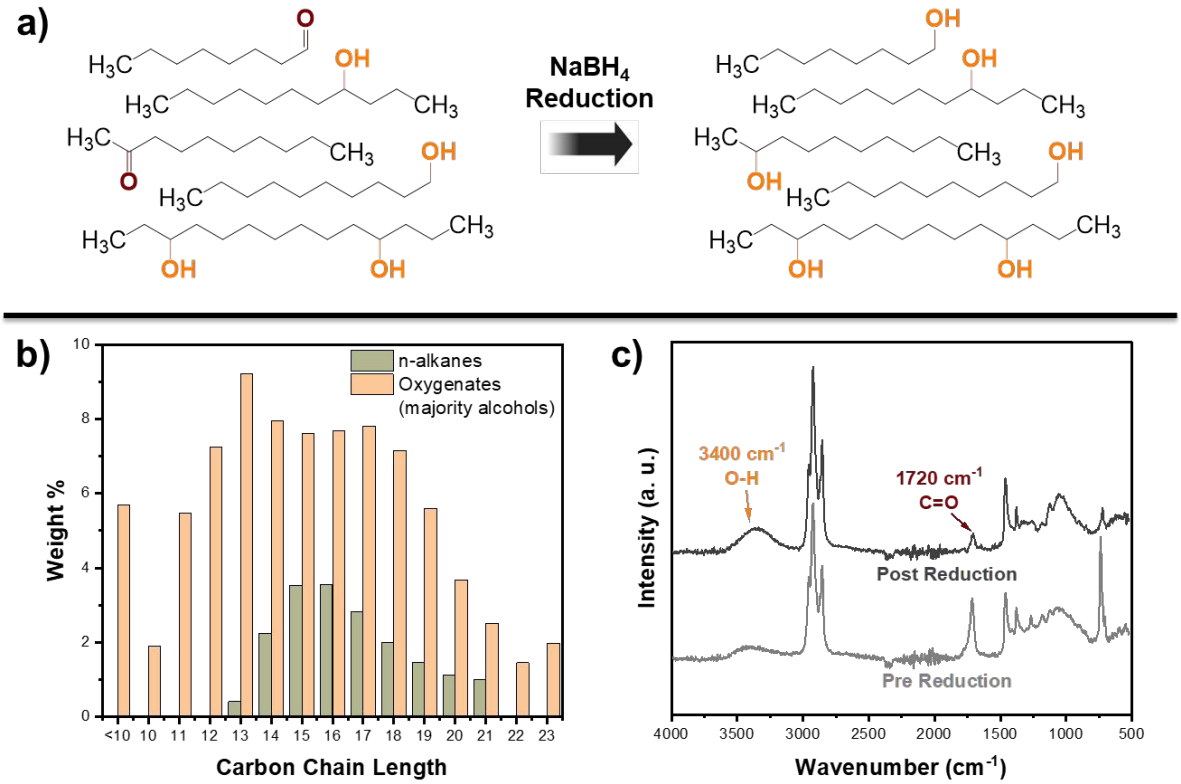

Figure 3. *(a) Schematic of $NaBH_4$ reduction of mixed plasma oxygenates to (mainly) alcohols. (b) Weight percent distribution of n-alkanes and oxygenates of post-reduced plasma-oxidized wax. (c) FTIR spectra of pre- and post-*

View Article Online
DOI: 10.1039/D6GC03112A

reduced plasma-oxidized wax. GC conditions: HP-Innowax column from 30 – 250 ºC in dichloromethane. FTIR conditions: MCTB detector at 4.0 cm^{-1} resolution and 32 scans.

Furoic Acid Esterification Reaction: PDHP to Plastics-Derived Furoates and Olefins (PDFO)

After successful reduction to mainly long-chain alcohols, the PDHP was processed with biomass-derived molecules, such as 2-furoic acid, to generate alkyl furoates, a valuable precursor to OFS (**Figure 4a**). However, due to the complexity of the PDHP mixture with various chain lengths and alcohol isomers and the possibility of side-product formation, optimization of the esterification process was conducted with model compounds. Screening of commercially available alcohols of varying chain length and OH group position demonstrated that secondary alcohols were more prone to acid-catalyzed dehydration to olefins (**Figure S8-9**). **Scheme S1** depicts the competing reaction pathways. Kinetic studies have shown that alcohol substitution is a key determinant of the selectivity of the dehydration reaction[38, 39] as the stability of the carbocation increases with the increasing number of electron-donating groups (i.e., CH_x groups). Additionally, alcohol groups positioned closer to the middle of the chain (i.e., 5-nonanol vs. 2-octanol) and similarly position alcohol groups with longer chains (i.e., 2-dodecanol vs. 2-octanol), exhibit lower conversion and higher olefin selectivity. This is likely due to reduced accessibility for nucleophilic attack on the protonated furoic acid[40] along with steric hindrance, thereby reducing activity and favoring dehydration over esterification. Therefore, to favor esterification over dehydration, optimization of the acid concentration (H_2SO_4) was conducted with 2-dodecanol (**Table S3** and **Figure S10**). Ester selectivity increased as acid loading decreased, as dehydration exhibits a higher acid concentration dependence[41-44] . Other Lewis acid catalysts, such as zinc oxide, chloride, and acetate, were screened for esterification; however, they resulted in low alcohol conversion compared to sulfuric acid (**Figure S11**).

After optimization, H_2SO_4 acid-catalyzed esterification with 2-furoic acid was conducted with the PDHP to generate plastic-derived furoates and olefins (PDFO). Products were identified and quantified via ^{1}H-NMR and GC-MS (**Figure 4b-c**). ^{1}H-NMR analysis (**Figure 4b**) indicated the reduction of the alcohol peak (~3.8-4 ppm), with the emergence of 3 distinct furan peaks (6-8 ppm), olefin peaks (5-5.5 ppm), and ester peak (4.2 ppm), indicative of the alkyl furoates and olefins synthesized. GC-MS analysis (**Figure 4c**) reveals the conversion of the PDHP to a mixture of olefins and furoates. The furoate products were confirmed by extraction of ion chromatograms corresponding to 95 m/z, a characteristic of the furoate ester group. A wide range of alkyl furoates from C_7 (MW 210 g/mol) to C_{23} (MW 434 g/mol) form, with the majority from the C_{12}-C_{17} alcohols, consistent with the distribution shown in **Figure 3b.** The estimated furoate yield was 21%, calculated using external standards of similar chain length, assuming the esters were all C_{14}, and the remaining yield was assumed to be olefins. Higher molecular weight compounds resulting from the acid-catalyzed oligomerization of olefins were not observed on the GC-MS[45]. However, a dark brown residue was observed in the reaction vial (approximately 0.1 g) which was insoluble in ethyl acetate as well as cyclohexane, indicating likely humins formation from the condensation of 2-furoic acid[46]. While the esterification reaction could use further optimization for higher furoate yields, the resulting PDFO (approximately 96% yield) is still favorable for surfactant production as a mixture of oleo-furan and branched sulfonates can have improved surfactant properties.

View Article Online
DOI: 10.1039/D6GC03112A

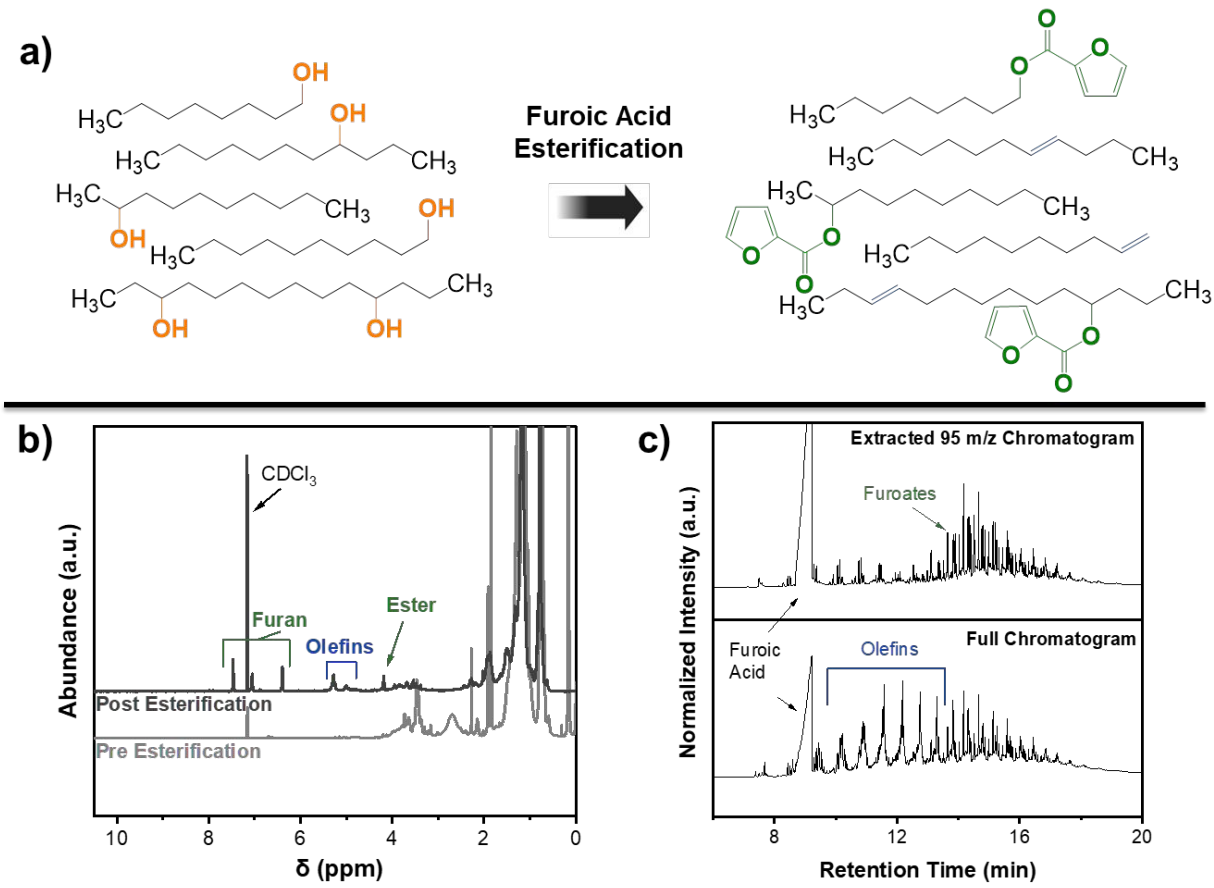

Figure 4. *(a) Schematic of furoic acid esterification of alcohols to furoates and olefins. (b) [1]H-NMR spectra of pre- and post-esterified plasma-oxidized alcohols. (c) Complete GC chromatogram and extracted 95 m/z ions chromatogram of post-esterified plasma-oxidized alcohols. [1]H-NMR conditions: 25 ºC in chloroform-d_2. GC conditions: HP-Innowax column from 30 – 250 ºC in dichloromethane.*

Sulfonation of PDFO to Plastics-Derived Oleo-furan and Branched Surfactants (PDOFBS)

The final step to obtain PDOFBS from PDFO involves the sulfonation of both furoates and olefins (**Figure 5a**). Sulfonation of the PDFO mixture and a standard octyl 2-furoate (O2F) was performed using chlorosulfonic acid. The PDFO mixture was sulfonated without prior separation, as previous studies have shown that olefins readily react with chlorosulfonic acid to form branched alkane and alkene sulfonates[47-49]. Notably, branched sulfonates have demonstrated promising surfactant properties[50, 51]. Furthermore, earlier OFS studies suggest that mixtures of oleo-furan sulfonates with other long-chain sulfonates can enhance surfactant performance, including lower CMC and Krafft temperatures. However, if pure OFS are needed, separation of furoates and olefins can be conducted via liquid-liquid extraction with polar and non-polar solvents (**Table S4**).

Successful sulfonation of the straight-chain O2F was confirmed by [1]H-NMR (**Figure 5b**), showing the disappearance of the alpha hydrogen signal (~7.6 ppm) on the furan ring, consistent with literature, as this position is the most reactive[52]. In contrast, the PDFO sulfonation displayed shifted furan peaks without complete disappearance of the alpha hydrogen, instead showing new furan signals upfield (**Figure 5c**). This suggests that sulfonation occurred at multiple sites across the various isomeric furoates. As with O2F, sulfonation can occur on the furan ring, leading to loss and shifting of characteristic peaks. Additionally, sulfonation may occur at the alpha carbon of the ester group[53, 54]. In the case of PDFO, where the esters are most likely branched, this carbon is

View Article Online
DOI: 10.1039/D6GC03112A

tertiary and more reactive, making it a likely sulfonation site. This results in a diminished ester peak (~4.2 ppm) while retaining the three original furan peaks (6-8 ppm). Altogether, the diverse isomeric furoates in PDFO give rise to a variety of sulfonated furoates. Additionally, the NMR spectra indicated evidence of olefins (5-5.5 ppm) and sulfate groups (3.8-4 ppm), which suggests the sulfonation of olefins to branched alpha olefin sulfonates and alkanesulfonates, which agrees with previous literature[47-49, 53, 54]. It should also be noted that the dissolution of the resulting products in D_2O provides further evidence of sulfonation, as unreacted compounds would not be soluble. Sulfonation conversions were calculated based on mass %, using the recovered unreacted furoates and olefins and assuming the remainder of the sample was successfully sulfonated, corresponding to 86.7% for O2F and 84.4% for PDFO, respectively. Overall, these results indicate the successful synthesis of OFS and branched sulfonates (PDOFBS) from biomass (2-furoic acid) and plastics waste (paraffins) derivatives.

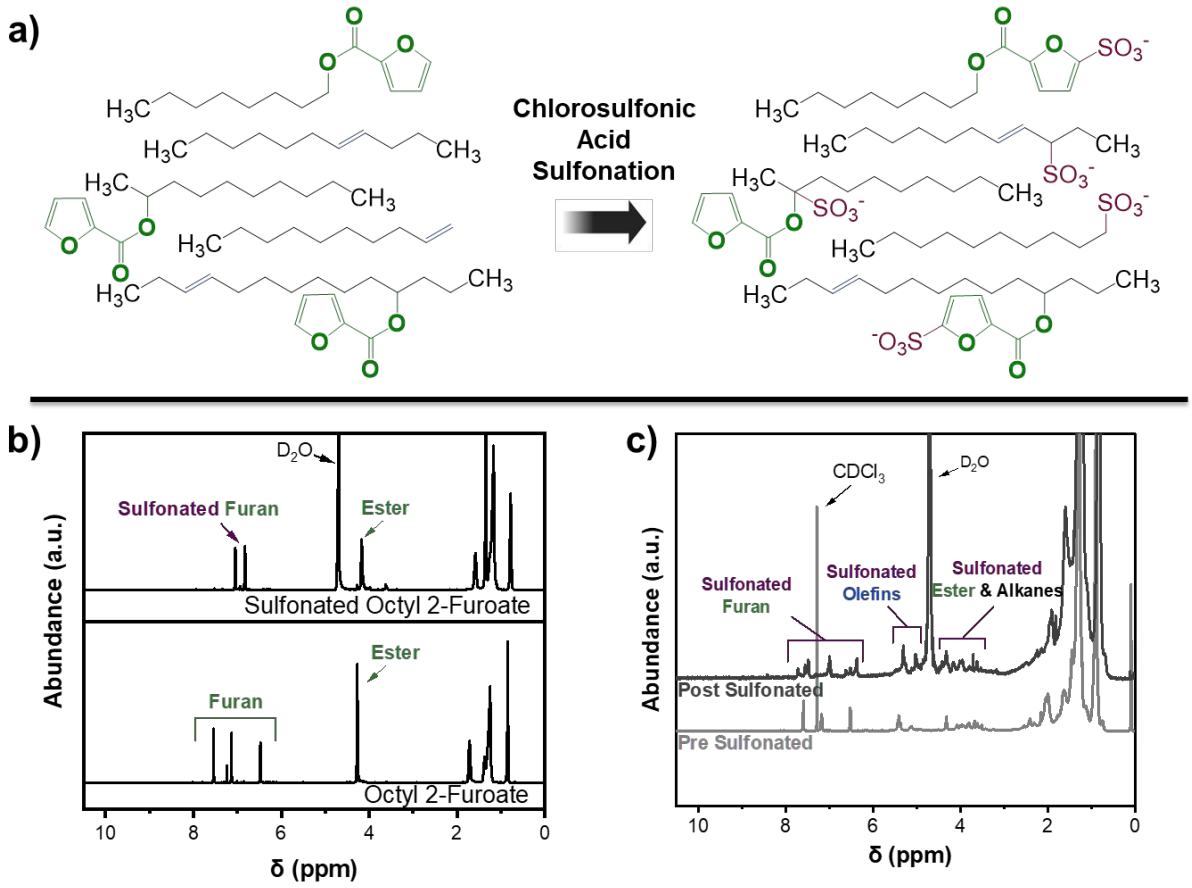

Figure 5. *(a) Schematic of chlorosulfonic acid sulfonation of furoates and olefins to mixed OFS and branched sulfonates. (b) ^{1}H-NMR spectra of pre- and post-sulfonated octyl 2-furoate standard. (c) ^{1}H-NMR spectra of pre- and post-sulfonated plastic-derived furoates and olefins. ^{1}H-NMR conditions: 25 ºC in chloroform-d_2 (pre-sulfonated) or deuterium oxide (post-sulfonated).*

Characterization of PDOFBS Surfactant

The two surfactants, standard sulfonated O2F and the PDOFBS, were characterized for two key properties: CMC and Krafft temperature. CMC refers to the minimum concentration at which surfactants self-assemble into micelles, while the Krafft temperature is the minimum temperature

View Article Online
DOI: 10.1039/D6GC03112A

above which surfactants remain soluble and can form micelles[8]. At room temperature (20 °C), the measured CMCs for sulfonated O2F (**Figure S12**) and the PDOFBS (**Figure 6a-b**) were 3533 ppm and 591 ppm, respectively. Notably, a previous study reported the CMC of sulfonated O2F as 1332 ppm[52]. The variation in values likely stems from differences in data interpretation and methods of calculating CMC from surface tension vs. concentration plots. Regardless, the PDOFBS exhibited a significantly lower CMC, likely due to its longer alkyl chains (C_{12}–C_{18}) compared to the octyl chain of O2F. The Krafft temperature of sulfonated O2F was determined to be below 0 °C, as no significant increase in conductivity was observed between 1 °C and 20 °C (**Figure S13**), consistent with prior findings. Surprisingly, the PDOFBS also exhibited a Krafft temperature below 0 °C despite its longer chains (**Figure 6c**). This behavior is likely due to the branched structures and the presence of a mixture of oleo-furan sulfonates and long-chain alkane and alpha olefin sulfonates, which enhance solubility at lower temperatures.

A comparison of CMC and Krafft temperature between the PDOFBS and previously reported oleo-furan sulfonates (OFS) and commercial surfactants is shown in **Figure 6d**. Ideal surfactants for aqueous applications exhibit low CMCs (< 2000 ppm) and Krafft temperatures (< 30 °C), with lower values indicating better performance. Previous OFS, including alkyl furans, furan ketones, and alkyl furoates, typically display tradeoffs: shorter chains yield lower Krafft temperatures but higher CMCs, whereas longer chains reduce CMCs but increase Krafft temperatures. The unique branched structures and mixed composition of the plastics-derived surfactants enable superior performance, outperforming not only previous OFS compounds but also commercial surfactants such as linear alkylbenzene sulfonate (LAS) and sodium lauryl sulfate (SLS). **Table S5** displays information on exact surfactants with corresponding CMC and Krafft temperature. Overall, these results demonstrate that surfactants derived from plastics waste and biomass could serve as high-performance, sustainable alternatives to conventional commercial surfactants.

View Article Online
DOI: 10.1039/D6GC03112A

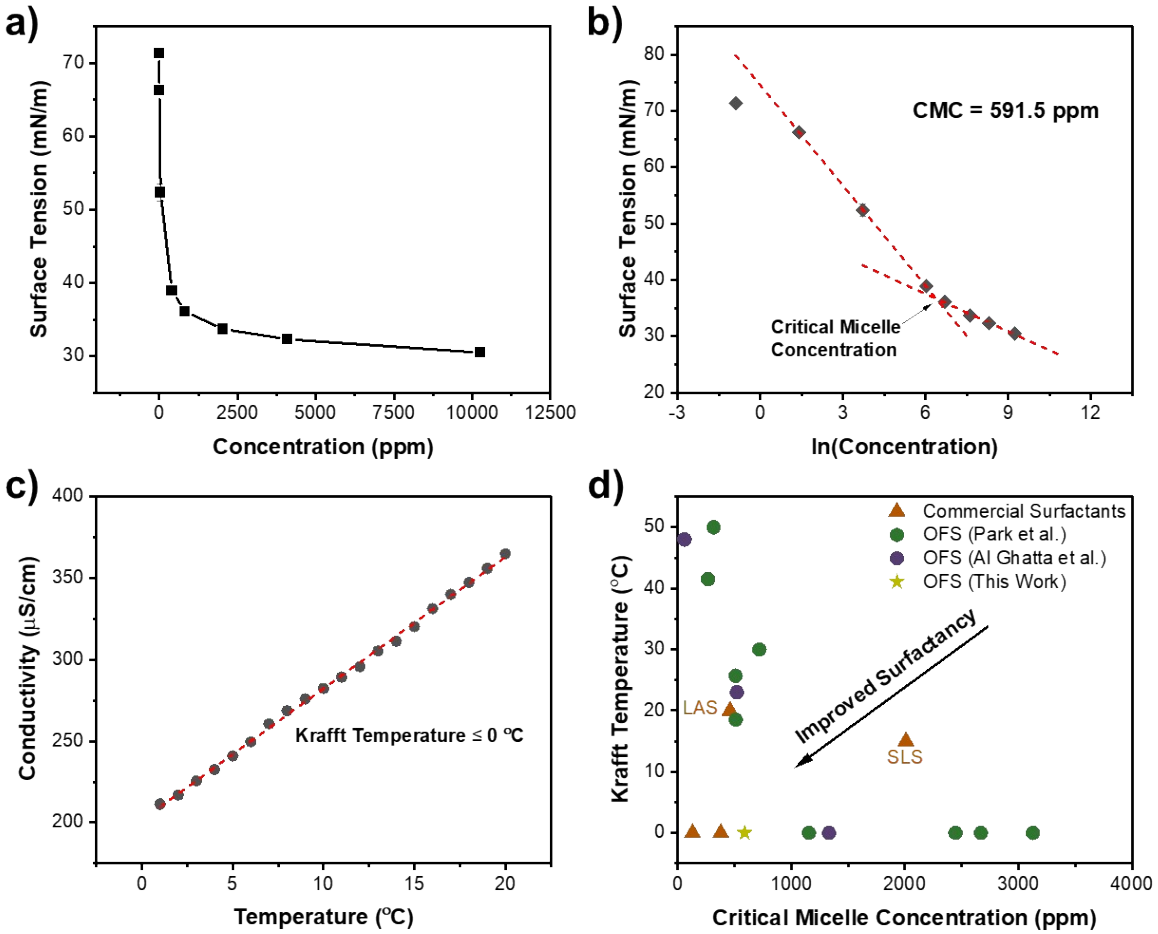

Figure 6. *(a) Surface tension vs. concentration plot of PDOFBS. (b) surface tension vs. ln(concentration) plot of PDOFBS with calculated CMC from the intersection of the sloped lines. (c) Conductivity at various temperatures of PDOFBS (842 ppm). (d) Comparison of Krafft temperature and CMC of PDOFBS to commercial and various OFS surfactants from previous works. Krafft temperatures marked at 0 indicates that surfactants formed micelles at the freezing point of water (0 °C) and temperatures below 0 were not measured.*

In terms of biodegradability and environmental persistence, toxicity simulations were conducted on C_{14} furoic ester (representing OFS), and C_{14} alkylbenzene (representing LAS) model compounds (**Table S6**). The aquatic toxicity results indicate that these OFS compounds are readily biodegradable compared to the C_{14} alkylbenzene, indicated by the lower bioconcentration factor (1.15 vs. 2.56). This behavior is attributed to the furan ring and ester group, which increase the likelihood of hydrolysis. Additionally, the OFS compounds exhibit higher water solubility (lower Log K_{ow}) and higher LC_{50} toward aquatic species (i.e., fathead minnow) than comparable industrial alkylbenzenes, providing an advantage in reducing environmental harm and persistence. However, the branched alkyl sulfonates mixed with the OFS are suggested to have similar biodegradation pathways as typical LAS and most likely exhibit similar aquatic toxicity[55].

Other key properties, such as detergency, emulsification, and foaming stability of the final products, require further testing and are crucial for evaluating the full practical applicability of these sustainable surfactants as replacements. These evaluations, along with optimization of the overall process, are planned for future work. The overall stability (hydrolytic, thermal, and oxidative) of these surfactants is also of interest. Based on the structures of the surfactants

View Article Online
DOI: 10.1039/D6GC03112A

(sulfonate group, branches, and furan ester ring), the furan ester ring appears to be the most reactive group. Compared to benzene rings (LAS surfactants), furan-based surfactants are expected to exhibit lower hydrolytic, thermal, and oxidative stability, reflecting a tradeoff with reduced environmental persistence. However, anionic furan-based surfactants have demonstrated relatively high hydrolytic stability over a broad pH range (basic, neutral, and mildly acidic), as hydroxide ions do not readily attack the negatively charged micelles of anionic surfactants[56]. Additionally, due to the unique mixture of both oleo-furan sulfonates and branched alkyl sulfonates, the overall hydrolytic, thermal, and oxidative stability may be closer to that of traditional LAS. Although further work is needed for a complete comparison, this study establishes a foundational synthetic route for producing OFS and branched surfactants from biomass and plastic waste.

CONCLUSIONS

This work presents a novel blueprint for producing sustainable surfactants through the co-processing of lignocellulosic biomass and post-consumer plastics. Specifically, inert polyolefin waste such as LDPE was converted into co-processable feedstocks via catalytic hydrogenolysis to paraffins, which were subsequently oxidized using an electrified non-thermal plasma process. These plastics-derived oxygenated paraffins were then selectively reduced and directly esterified with biobased 2-furoic acid to produce long-chain furoates and olefins. Sulfonation of these intermediates yielded a unique mixture of oleo-furan and branched sulfonate surfactants. Compared to commercial and purely biomass-derived surfactants, the resulting hybrid feedstock-derived surfactants exhibit excellent performance, including low CMC and low Krafft temperature. This integrated approach, combining plasma-enabled oxidation with organic transformations, offers a general strategy for generating reactive intermediates from plastics waste. However, expanding this process to mixed plastic waste, which can include additives, fillers, and other contaminants, could lead to many detrimental effects, such as catalyst deactivation during hydrogenolysis, formation of undesired side-products during plasma oxidation, and decreased selectivity and yields during downstream transformation (reduction, esterification, and sulfonation). Therefore, future work will focus on utilizing mixed plastic waste (mixed feedstocks and additives), understanding their effects on overall upcycling via this synthetic route, and optimizing the route to handle these mixed streams.

In terms of the practicality of large-scale surfactant production, an overall process efficiency analysis (Table S7) and a preliminary cost analysis (Table S8) have been conducted for this multi-step process system, accounting for the operating costs of each step. In terms of yield efficiency, this entire process scheme can generate 0.31 mols of PDOFBS surfactants for every 1 mol of LDPE plastic waste (31% overall efficiency). Assuming the total reagent costs are approximately 80% of total production costs and neglecting capital and operating costs for separations, the breakeven cost of the synthesized surfactants is estimated at \$3.12/kg. If these materials were to replace linear alkylbenzene sulfonates (LAS), which currently sell for approximately \$1.80/kg, the process would operate at a \$1.32/kg deficit. The plasma reactor is the largest contributor to operating costs, accounting for approximately 52% of the total cost due to the electrical energy required to generate the oxygen plasma, and it has the lowest efficiency (52%). These calculations are based on this specific reaction and reactor, where the plasma power dissipation is 2.2 W, corresponding to an energy efficiency of 1.7×10^{-8} kg/J. Assuming a U.S. electricity cost of \$0.17/kWh, the plasma cost of oxidizing long-chain alkanes into oxygenated hydrocarbons is approximately \$2.84/kg (\$1.63/kg surfactant). However, this energy and yield efficiency can further be improved through plasma reactor optimization. Optimizing the reactor geometry to increase the plasma-liquid

View Article Online
DOI: 10.1039/D6GC03112A

interface, such as bubbling or use of microfluidics, can decrease the required treatment time, increase the production rate, and increase energy efficiency[31, 57]. Additionally, due to the relatively simple and smaller configuration, a numbering-up strategy is well-suited for scale-up, such as an array of pins impinging on a liquid surface or employing multiple plasma reactors in parallel, to increase production rates[58]. Although the overall process is currently not economically feasible for large-scale surfactant synthesis based on this preliminary techno-economic analysis (TEA) and overall process efficiency analysis, it demonstrates a synthetic blueprint for converting plastic and biomass waste into surfactants. This framework can be further developed and optimized to improve scalability and economic viability in future work. Overall, this process demonstrates the feasibility of uniting biomass valorization and plastics upcycling into a single synthetic framework, enabling the production of high-performance materials without reliance on new fossil carbon.

ACKNOWLEDGMENTS

The plasma work of D.K.N. was supported by the U.S. National Science Foundation under award number 2134471. His earlier plasma work was supported as part of the Center for Plastics Innovation, an Energy Frontier Research Center funded by the US Dept. of Energy, Office of Science, Office of Basic Energy Sciences under award number DE-SC0021166. The organic transformation work of T.G. was supported as part of the Delaware Biosciences Center for Advanced Technology grant with award number 12A00448.

AUTHOR CONTRIBUTIONS

Conceptualization: TG, DKN, DGV
Methodology: TG, DKN, DGV
Investigation: TG, DKN, MAAI, CK
Visualization: TG, DKN
Funding acquisition: DGV
Project administration: DGV
Supervision: DGV
Writing – original draft: TG, DKN, MAAI, CK
Writing – review & editing: TG, DKN, MAAI, CK, DGV

DECLARATION OF COMPETING INTEREST

The authors have a patent application for this process.

SUPPORTING INFORMATION

The supporting information is available free of charge.

Electrical waveforms; optical emission spectroscopy spectrum; C_{16} proof of concept and stability experiments; GC analysis of post-plasma-oxidized paraffins and gas trap; Pd/C hydrogenation model compound results; $NaBH_4$ reduction model compound results; GC and NMR results of post-reduced oxygenated paraffins; esterification screening of primary and secondary alcohols; time-dependent esterification of varying secondary alcohol position and chain length; schematic of esterification reaction; optimization of acid concentration for esterification; lewis acid screening for esterification; solvent extraction for esters and olefins; surface tension vs concentration plots for O2F; conductivity vs temperature for O2F; comparison table for previous OFS and commercial surfactants.

View Article Online
DOI: 10.1039/D6GC03112A

REFERENCES

(1) Tilsted, J. P.; Bauer, F.; Deere Birkbeck, C.; Skovgaard, J.; Rootzén, J. Ending fossil-based growth: Confronting the political economy of petrochemical plastics. *One Earth* **2023**, *6* (6), 607-619. DOI: https://doi.org/10.1016/j.oneear.2023.05.018.
(2) Research, G. V. *Specialty Chemicals Market Size, Share & Trends Analysis Report By Product (Institutional & Industrial Cleaners, Flavor & Fragrances, Food & Feed Additives), By Application, By Region, And Segment Forecasts, 2024–2030*. 2024. https://www.grandviewresearch.com/industry-analysis/specialty-chemicals-market (accessed.
(3) Research, T. M. *Linear Alkyl Benzene (LAB) Market- Global Industry Analysis and Forecast 2012-2018*. 2021. https://www.transparencymarketresearch.com/linear-alkyl-benzene-market.html (accessed.
(4) Nakama, Y. Chapter 15 - Surfactants. In *Cosmetic Science and Technology*, Sakamoto, K., Lochhead, R. Y., Maibach, H. I., Yamashita, Y. Eds.; Elsevier, 2017; pp 231-244.
(5) Yadav, G. D.; Doshi, N. S. Synthesis of Linear Phenyldodecanes by the Alkylation of Benzene with 1-Dodecene over Non-Zeolitic Catalysts. *Organic Process Research & Development* **2002**, *6* (3), 263-272. DOI: 10.1021/op000044s.
(6) Kocal, J. A.; Vora, B. V.; Imai, T. Production of linear alkylbenzenes. *Applied Catalysis A: General* **2001**, *221* (1), 295-301. DOI: https://doi.org/10.1016/S0926-860X(01)00808-0.
(7) Jensen, J. Fate and effects of linear alkylbenzene sulphonates (LAS) in the terrestrial environment. *Sci Total Environ* **1999**, *226* (2-3), 93-111. DOI: 10.1016/s0048-9697(98)00395-7 From NLM.
(8) Park, D. S.; Joseph, K. E.; Koehle, M.; Krumm, C.; Ren, L.; Damen, J. N.; Shete, M. H.; Lee, H. S.; Zuo, X.; Lee, B.; et al. Tunable Oleo-Furan Surfactants by Acylation of Renewable Furans. *ACS Cent Sci* **2016**, *2* (11), 820-824. DOI: 10.1021/acscentsci.6b00208 From NLM.
(9) Al Ghatta, A.; Perry, J. M.; Maeng, H.; Lemus, J.; Hallett, J. P. Sustainable and efficient production of furoic acid from furfural through amine assisted oxidation with hydrogen peroxide and its implementation for the synthesis of alkyl furoate. *RSC Sustainability* **2023**, *1* (2), 303-309. DOI: 10.1039/d2su00102k.
(10) Deng, F.; Amarasekara, A. S. Catalytic upgrading of biomass derived furans. *Industrial Crops and Products* **2021**, *159*, 113055. DOI: https://doi.org/10.1016/j.indcrop.2020.113055.
(11) Dijkstra, A. J. Lauric Oils. In *Encyclopedia of Food and Health*, Caballero, B., Finglas, P. M., Toldrá, F. Eds.; Academic Press, 2016; pp 517-522.
(12) Ezigbo, V. O.; Emmanuella, A. Extraction of lauric acid from coconut oil, its applications and health implications on some microorganisms. *Afr J Educ Sci Technol* **2016**, *3* (3), 144-147.
(13) Goculdas, T.; Yuliu, Z.; Sadula, S.; Zheng, W.; Saha, B.; Nanduri, A.; Ierapetritou, M.; Vlachos, D. G. Process intensified lauric acid self-ketonization and its economic and environmental impact on biolubricant base oil production. *Green Chemistry* **2024**, *26* (15), 8818-8830, 10.1039/D4GC01721H. DOI: 10.1039/D4GC01721H.
(14) Goculdas, T.; Deshpande, S.; Zheng, W.; Gorte, R. J.; Sadula, S.; Vlachos, D. G. Highly selective cross ketonization of renewable acids over magnesium oxide. *Green Chemistry* **2023**, *25* (2), 614-626, 10.1039/D2GC04400E. DOI: 10.1039/D2GC04400E.
(15) Wang, H.; Huang, S.; Tsang, S. C. E. Heterogeneous catalysis strategies for polyolefin plastic upcycling: co-reactant-assisted and direct transformation under mild conditions. *Chemical Communications* **2025**, *61* (8), 1496-1508. DOI: 10.1039/d4cc05471g.
(16) Agency, U. S. E. P. *Facts and Figures about Materials, Waste and Recycling*. 2025. https://www.epa.gov/facts-and-figures-about-materials-waste-and-recycling (accessed.

View Article Online
DOI: 10.1039/D6GC03112A

(17) Lee, K.; Jing, Y.; Wang, Y.; Yan, N. A unified view on catalytic conversion of biomass and waste plastics. *Nature Reviews Chemistry* **2022**, *6* (9), 635-652. DOI: 10.1038/s41570-022-00411-8.
(18) Bachmann, M.; Zibunas, C.; Hartmann, J.; Tulus, V.; Suh, S.; Guillén-Gosálbez, G.; Bardow, A. Towards circular plastics within planetary boundaries. *Nature Sustainability* **2023**, *6* (5), 599-610. DOI: 10.1038/s41893-022-01054-9.
(19) Li, H.; Aguirre-Villegas, H. A.; Allen, R. D.; Bai, X.; Benson, C. H.; Beckham, G. T.; Bradshaw, S. L.; Brown, J. L.; Brown, R. C.; Cecon, V. S.; et al. Expanding plastics recycling technologies: chemical aspects, technology status and challenges. *Green Chemistry* **2022**, *24* (23), 8899-9002. DOI: 10.1039/d2gc02588d.
(20) Lopez, G.; Artetxe, M.; Amutio, M.; Bilbao, J.; Olazar, M. Thermochemical routes for the valorization of waste polyolefinic plastics to produce fuels and chemicals. A review. *Renewable and Sustainable Energy Reviews* **2017**, *73*, 346-368. DOI: https://doi.org/10.1016/j.rser.2017.01.142.
(21) Banu, J. R.; Sharmila, V. G.; Ushani, U.; Amudha, V.; Kumar, G. Impervious and influence in the liquid fuel production from municipal plastic waste through thermo-chemical biomass conversion technologies - A review. *Science of The Total Environment* **2020**, *718*, 137287. DOI: https://doi.org/10.1016/j.scitotenv.2020.137287.
(22) Kots, P. A.; Vance, B. C.; Vlachos, D. G. Polyolefin plastic waste hydroconversion to fuels, lubricants, and waxes: a comparative study. *Reaction Chemistry & Engineering* **2022**, *7* (1), 41-54, 10.1039/D1RE00447F. DOI: 10.1039/D1RE00447F.
(23) Liu, S.; Kots, P. A.; Vance, B. C.; Danielson, A.; Vlachos, D. G. Plastic waste to fuels by hydrocracking at mild conditions. *Science Advances* **2021**, *7* (17), eabf8283. DOI: 10.1126/sciadv.abf8283.
(24) Shi, J. X.; Ciccia, N. R.; Pal, S.; Kim, D. D.; Brunn, J. N.; Lizandara-Pueyo, C.; Ernst, M.; Haydl, A. M.; Messersmith, P. B.; Helms, B. A.; et al. Chemical Modification of Oxidized Polyethylene Enables Access to Functional Polyethylenes with Greater Reuse. *Journal of the American Chemical Society* **2023**, *145* (39), 21527-21537. DOI: 10.1021/jacs.3c07186.
(25) Kots, P. A.; Liu, S.; Vance, B. C.; Wang, C.; Sheehan, J. D.; Vlachos, D. G. Polypropylene Plastic Waste Conversion to Lubricants over Ru/TiO2 Catalysts. *ACS Catalysis* **2021**, *11* (13), 8104-8115. DOI: 10.1021/acscatal.1c00874.
(26) Nguyen, D. K.; Dimitrakellis, P.; Talley, M. R.; O'Dea, R. M.; Epps, T. H., III; Watson, M. P.; Vlachos, D. G. Oxidative Functionalization of Long-Chain Liquid Alkanes by Pulsed Plasma Discharges at Atmospheric Pressure. *ACS Sustainable Chemistry & Engineering* **2022**, *10* (48), 15749-15759. DOI: 10.1021/acssuschemeng.2c04269.
(27) Li, S.; Tang, Z.; Zhou, F.; Li, W.; Yuan, X. Separation of Primary Alcohols and Saturated Alkanes from Fisher–Tropsch Synthesis Products. *Chinese Journal of Chemical Engineering* **2014**, *22* (9), 980-983. DOI: https://doi.org/10.1016/j.cjche.2014.06.025.
(28) Brown, H. C.; Mead, E. J.; Subba Rao, B. C. A Study of Solvents for Sodium Borohydride and the Effect of Solvent and the Metal Ion on Borohydride Reductions1. *Journal of the American Chemical Society* **1955**, *77* (23), 6209-6213. DOI: 10.1021/ja01628a044.
(29) Tamura, M.; Miyaoka, S.; Nakaji, Y.; Tanji, M.; Kumagai, S.; Nakagawa, Y.; Yoshioka, T.; Tomishige, K. Structure-activity relationship in hydrogenolysis of polyolefins over Ru/support catalysts. *Applied Catalysis B: Environmental* **2022**, *318*, 121870. DOI: https://doi.org/10.1016/j.apcatb.2022.121870.

View Article Online
DOI: 10.1039/D6GC03112A

(30) Wandell, R. J.; Locke, B. R. Hydrocarbon Processing by Plasma. Springer International Publishing, 2017; pp 1163-1182.
(31) Nguyen, D. K.; Cameli, F.; Dimitrakellis, P.; Vlachos, D. G. Biphasic Plasma Microreactor for Oxyfunctionalization of Liquid Hydrocarbons. *Industrial & Engineering Chemistry Research* **2024**, *63* (20), 9008-9017. DOI: 10.1021/acs.iecr.4c00605.
(32) Patiño, P.; Méndez, M.; Pastrán, J.; Gambús, G.; Navea, J.; Escobar, O.; Castro, A. Oxidation of Cycloalkanes and Diesel Fuels by Means of Oxygen Low Pressure Plasmas. *Energy & Fuels* **2002**, *16* (6), 1470-1475. DOI: 10.1021/ef020068v.
(33) Gambús, G.; Patiño, P.; Méndez, B.; Sifontes, A.; Navea, J.; Martín, P.; Taylor, P. Oxidation of Long Chain Hydrocarbons by Means of Low-Pressure Plasmas. *Energy & Fuels* **2001**, *15* (4), 881-886. DOI: 10.1021/ef000271v.
(34) Patiño, P.; Hernández, F. E.; Rondón, S. Reactions of O(3P) with secondary C-H bonds of saturated hydrocarbons in nonequilibrium plasmas. *Plasma Chemistry and Plasma Processing* **1995**, *15* (2), 159-171. DOI: 10.1007/BF01459694.
(35) Patiño, P.; Mejía, A.; Rodríguez, P.; Méndez, B. Upgrading of diesel fuels and mixtures of hydrocarbons by means of oxygen low pressure plasmas: a comparative study☆. *Fuel* **2003**, *82* (13), 1613-1619. DOI: https://doi.org/10.1016/S0016-2361(03)00076-0.
(36) Wu, L.; Moteki, T.; Amit; David; Toste, F. D. Production of Fuels and Chemicals from Biomass: Condensation Reactions and Beyond. *Chem* **2016**, *1* (1), 32-58. DOI: 10.1016/j.chempr.2016.05.002.
(37) Sekerová, L.; Spáčilová, M.; Vyskočilová, E.; Krupka, J.; Červený, L. Acid catalyzed acetalization of aldehydes with diols resulting into the formation of fragrant cyclic acetals. *Reaction Kinetics, Mechanisms and Catalysis* **2019**, *127* (2), 727-740. DOI: 10.1007/s11144-019-01595-9.
(38) Zimmermann, H.; Rudolph, J. Protonic States and the Mechanism of Acid-Catalysed Esterification. *Angewandte Chemie International Edition in English* **1965**, *4* (1), 40-49. DOI: 10.1002/anie.196500401.
(39) Tran, B.; Milner, S. T.; Janik, M. J. Kinetics of Acid-Catalyzed Dehydration of Alcohols in Mixed Solvent Modeled by Multiscale DFT/MD. *ACS Catalysis* **2022**, *12* (21), 13193-13206. DOI: 10.1021/acscatal.2c03978.
(40) Sahu, A.; Pandit, A. B. Kinetic Study of Homogeneous Catalyzed Esterification of a Series of Aliphatic Acids with Different Alcohols. *Industrial & Engineering Chemistry Research* **2019**, *58* (8), 2672-2682. DOI: 10.1021/acs.iecr.8b04781.
(41) Smith, H. A. Kinetics of the Catalyzed Esterification of Normal Aliphatic Acids in Methyl Alcohol. *Journal of the American Chemical Society* **1939**, *61* (2), 254-260. DOI: 10.1021/ja01871a011.
(42) Neveu, C. D.; Sondjaja, R.; Stöhr, T.; Iroff, N. J. 10.26 - Lubricant and Fuel Additives Based on Polyalkylmethacrylates. In *Polymer Science: A Comprehensive Reference*, Matyjaszewski, K., Möller, M. Eds.; Elsevier, 2012; pp 453-478.
(43) Bart, H. J.; Reidetschläger, J.; Schatka, K.; Lehmann, A. Kinetics of esterification of succinic anhydride with methanol by homogeneous catalysis. *International Journal of Chemical Kinetics* **1994**, *26* (10), 1013-1021. DOI: 10.1002/kin.550261006.
(44) Krzelj, V.; Ferreira Liberal, J.; Papaioannou, M.; van der Schaaf, J.; Neira d'Angelo, M. F. Kinetic Model of Xylose Dehydration for a Wide Range of Sulfuric Acid Concentrations. *Industrial & Engineering Chemistry Research* **2020**, *59* (26), 11991-12003. DOI: 10.1021/acs.iecr.0c01197.

View Article Online
DOI: 10.1039/D6GC03112A

(45) Nicholas, C. P. Applications of light olefin oligomerization to the production of fuels and chemicals. *Applied Catalysis A: General* **2017**, *543*, 82-97. DOI: https://doi.org/10.1016/j.apcata.2017.06.011.
(46) Shi, N.; Liu, Q.; Ju, R.; He, X.; Zhang, Y.; Tang, S.; Ma, L. Condensation of α-Carbonyl Aldehydes Leads to the Formation of Solid Humins during the Hydrothermal Degradation of Carbohydrates. *ACS Omega* **2019**, *4* (4), 7330-7343. DOI: 10.1021/acsomega.9b00508.
(47) Roberts, D. W.; Williams, D. L. Sultones as By-Products in Anionic Surfactants. *Tenside Surfactants Detergents* **1983**, *20* (3), 109-111. DOI: doi:10.1515/tsd-1983-200308 (acccessed 2025-05-18).
(48) Bakker, B. H.; Cerfontain, H. Sulfonation of Alkenes by Chlorosulfuric Acid, Acetyl Sulfate, and Trifluoroacetyl Sulfate. *European Journal of Organic Chemistry* **1999**, *1999* (1), 91-96. DOI: https://doi.org/10.1002/(SICI)1099-0690(199901)1999:1<91::AID-EJOC91>3.0.CO;2-J.
(49) Miron, S.; Richter, G. H. Sulfonation of 2-Pentene by Chlorosulfonic Acid. *Journal of the American Chemical Society* **1949**, *71* (2), 453-455. DOI: 10.1021/ja01170a022.
(50) Li, X.; Li, J.; Wang, X.; Yang, L.; Xu, H.; Dong, J. Novel branched-chain sulfonate surfactants based on α-olefins from Fischer–Tropsch synthesis via reaction-separation-utilization integrated process. *Fuel* **2023**, *339*, 126961. DOI: https://doi.org/10.1016/j.fuel.2022.126961.
(51) Wang, Y.; Liu, X.; Bai, L.; Niu, J. Influence of alkyl chain length of alpha olefin sulfonates on surface and interfacial properties. *Journal of Dispersion Science and Technology* **2017**, *38* (12), 1764-1769. DOI: 10.1080/01932691.2017.1281144.
(52) Al Ghatta, A.; Aravenas, R. C.; Wu, Y.; Perry, J. M.; Lemus, J.; Hallett, J. P. New Biobased Sulfonated Anionic Surfactants Based on the Esterification of Furoic Acid and Fatty Alcohols: A Green Solution for the Replacement of Oil Derivative Surfactants with Superior Proprieties. *ACS Sustainable Chemistry & Engineering* **2022**, *10* (27), 8846-8855. DOI: 10.1021/acssuschemeng.2c01766.
(53) Xie, T.; Zeng, C.; Wang, C.; Zhang, L. Preparation of Methyl Ester Sulfonates Based on Sulfonation in a Falling Film Microreactor from Hydrogenated Palm Oil Methyl Esters with Gaseous SO3. *Industrial & Engineering Chemistry Research* **2013**, *52* (10), 3714-3722. DOI: 10.1021/ie3028763.
(54) Stein, W.; Baumann, H. α-Sulfonated fatty acids and esters: Manufacturing process, properties, and applications. *Journal of the American Oil Chemists Society* **1975**, *52* (9), 323-329. DOI: 10.1007/BF02639188.
(55) Scott, M. J.; Jones, M. N. The biodegradation of surfactants in the environment. *Biochimica et Biophysica Acta (BBA) - Biomembranes* **2000**, *1508* (1), 235-251. DOI: https://doi.org/10.1016/S0304-4157(00)00013-7.
(56) Lundberg, D.; Stjerndahl, M.; Holmberg, K. Ester-based surfactants: Are they stable enough? *Journal of Surfactants and Detergents* **2023**, *26* (3), 229-236. DOI: https://doi.org/10.1002/jsde.12628 (acccessed 2026/03/10).
(57) Bruggeman, P. J.; Kushner, M. J.; Locke, B. R.; Gardeniers, J. G. E.; Graham, W. G.; Graves, D. B.; Hofman-Caris, R. C. H. M.; Maric, D.; Reid, J. P.; Ceriani, E.; et al. Plasma–liquid interactions: a review and roadmap. *Plasma Sources Science and Technology* **2016**, *25* (5), 053002. DOI: 10.1088/0963-0252/25/5/053002.
(58) Burlica, R.; Cretu, D.-E.; Beniuga, O.; Astanei, D. Nonthermal Plasma Multi-Reactor Scale-Up Using Pulse Capacitive Power Supplies. *Applied Sciences* **2022**, *12* (20), 10403.

View Article Online
DOI: 10.1039/D6GC03112A

View Article Online
DOI: 10.1039/D6GC03112A

All key data is provided in the manuscript or supplementary information. For additional information may be requested from the corresponding author.